International Journal of GEOMATE, Dec, 2022, Vol.23, Issue 100, pp.102-109
ISSN: 2186-2982 (P), 2186-2990 (O), Japan, DOI: https://doi.org/10.21660/2022.100.g12121
Geotechnique, Construction Materials and Environment

S1-PSINSAR MONITORING AND HYPERBOLIC MODELING OF NONLINEAR GROUND SUBSIDENCE IN NAGA CITY, CEBU ISLAND IN THE PHILIPPINES

*Ryan A. Ramirez[1,2], Rajiv Eldon E. Abdullah[1] and Christabel Jane P. Rubio[1,2]

[1]Faculty of Engineering, University of Santo Tomas, Manila 1015, Philippines; [2]National Research Council of the Philippines, Taguig 1631, Philippines

*Corresponding Author, Received: 04 March 2022, Revised: 06 Dec. 2022, Accepted: 15 Dec. 2022

ABSTRACT: Human activities are increasingly altering subsurface conditions leading to unwanted ground deformations. Excessive ground deformations endanger buildings, linear systems, underground facilities, and, ultimately, people's safety. Thus, mapping and monitoring ground deformation are critical in managing disaster risk and mitigating socio-economic damage from possible geohazards. Accessible and archived satellite data and the continual development of advanced remote sensing technologies can now provide valuable information about the earth's surface for various applications. This study applied the descending Sentinel-1 Persistent Scatterer Interferometric Synthetic Aperture Radar (S1-PSInSAR) technique for long-term remote ground deformation monitoring over the coastal city of Naga in Cebu Island in the Philippines. The S1-PSInSAR technique provided relatively dense ground monitoring points, specifically over built-up areas. The maximum ground subsidence along the radar line-of-sight (LOS) estimated throughout the monitoring period from October 2014 to September 2018 exceeds –50 mm, whereas the LOS mean displacement velocity exceeds –15 mm/yr. The two-parameter hyperbolic model well fitted the S1-PSInSAR results to describe the ground deformation's non-uniform and nonlinear behavior. Ground deformation over the coastal city continues to evolve, and stabilization is yet to occur. This study suggests that the S1-PSInSAR technique and the hyperbolic function can provide technical support in mapping, monitoring, and (or) forecasting ground deformation over vast areas with less human labor and efficient cost.

Keywords: Sentinel-1 PSInSAR, Ground deformation monitoring, Hyperbolic model, Coastal city, Cebu Island

1. INTRODUCTION

Reclamation projects along coastal cities for industrial, residential, and commercial use have allowed land expansions. Human activities aiding continual urban sprawl over reclaimed lands and the current sea level rise, coastal erosion, and underground resource extraction are increasingly altering subsurface conditions resulting in unwanted ground deformations. Excessive ground deformations endanger structures, linear systems, underground facilities, and, ultimately, people's safety. Thus, ground deformation mapping and long-term monitoring over coastal cities are critical to prevent disaster risk and mitigate socio-economic damage from such geohazards [1].

Ground-based geodetic methods such as precise leveling and terrestrial measurements such as Global Positioning System (GPS) are standard monitoring methods providing accurate and reliable ground deformation [2]–[3]. However, these methods are inefficient to deploy over vast areas and long-term because of the workforce needed and the high cost associated. Meanwhile, accessible and archived satellite Synthetic Aperture Radar (SAR) data and the continual development of advanced remote sensing techniques have emerged as viable solutions for geohazard mitigation. The launch of the Sentinel-1 (S1) mission under the Copernicus Program of the European Space Agency (ESA) and European Commission (EC) has provided accessible SAR data since 2014, which the scientific community is enjoying for various earth and geoinformation applications. Specifically, the Persistent Scatterer Interferometric SAR (PSInSAR) has been successfully applied across multiple geohazard applications [4]. Theoretical and technical reviews of different PSInSAR algorithms are available in the literature [5]–[6]. PSInSAR provided the opportunity to detect, map, and monitor ground deformations along the coasts caused or enhanced by natural and anthropic activities [7]–[12]. In low-lying coastal urban areas in Metro Manila, the Philippines, ground deformation from 1993-to-2010 and 2015-to-2019 has been investigated using differential InSAR (DInSAR) and PSInSAR, respectively [13]–[14]. Nevertheless, limited studies are available in the literature exploiting the S1-PSInSAR technique in other coastal cities in the Philippines experiencing short- to long-term nonlinear ground deformations reflecting the complex interaction among natural

and anthropic processes. Specifically, free and accessible archived SAR datasets are not widely exploited in the Philippines, despite the country facing various geohazard types besides ground subsidence (i.e., flooding, landslides, volcano eruption, and earthquakes) [15]–[19].

This study applied the S1-PSInSAR technique for long-term remote ground deformation monitoring over the coastal city of Naga in Cebu Island in the Philippines using descending S1 SAR dataset acquired between October 2014 and September 2018. The cumulative line-of-sight (LOS) displacement obtained from the S1-PSInSAR analysis was modeled using a two-parameter hyperbolic model to describe the non-uniform and nonlinear ground deformation process over a multipurpose complex zone built over reclaimed land in Naga city.

2. RESEARCH SIGNIFICANCE

This research provides a cost-efficient, non-intrusive satellite-based geodetic monitoring tool leveraging free-to-use S1 SAR satellite data. This monitoring tool is critical to appropriately appraise buildings and infrastructure damage due to non-uniform and nonlinear urban ground subsidence in an active and dynamic, developed environment, like coastal cities in the Philippines. Accordingly, the S1-PSInSAR technique applied in this study can be extended to encompass and test the potential of future remote sensing data to be acquired by planned SAR satellites to be developed and operated by the Philippine Space Agency (PhilSA).

3. STUDY AREA AND S1 SAR DATASET

3.1 Study Area

Cebu Island's geological structure comprises a Jurassic-Cretaceous igneous and metamorphic basement complex and Cenozoic sedimentary and volcanic rock units [20]–[21]. The island is classified as a tropical rainforest [22]. The Philippine Atmospheric, Geophysical and Astronomical Services Administration (PAGASA 2022) reported a mean annual rainfall of 1,565 mm for Cebu Island. Naga city is located on the southeastern coast of Cebu Island, characterized by karst terrain. Ridges and valleys converged to a coastal plain in the southeast part of the city. Land use is predominantly cultivated lands with quarry zones. Small villages are located inland, whereas built-up areas are concentrated mainly along the coastal plain. The nearest potentially active faults are the South and Central Cebu faults; the latter passes through Naga city. Between October 2014 and September 2018, the Philippine Institute of Volcanology and Seismology (PHIVOLCS 2018) recorded one earthquake of magnitude 5.2, 7 earthquakes of magnitude between 4 and 5, 45 earthquakes of magnitude between 3 and 4, and 173 earthquakes of magnitude between 2 and 3 that shook Cebu Island. There were also 14 earthquakes with a magnitude below 2.

3.2 S1 SAR Dataset

The S1 mission acquired the SAR dataset exploited in this study. The S1 mission consists of two right-side-looking satellites: S1-A, launched on April 3, 2014, and S1-B, launched on April 25, 2016. S1 sensors operate at a wavelength λ equal to 5.6 cm (C-band). The twin constellation has a near-polar sun-synchronous orbit with a 6–12 days repeat cycle over the exact location. S1 SAR products acquired in the interferometric wide swath mode have a ground range coverage of approximately 250 km, thanks to the Terrain Observation by Progressive Scans (TOPS) mode [23]. The geometric resolution in the range and azimuth directions is 5 m × 20 m, respectively.

This study collected 139 S1 single-look complex SAR images from October 21, 2014, to September 18, 2018. The images were acquired by the S1 descending satellite (track 61), whose flight is from north to south. The minimum and maximum time gap between each successive image are 6 and 48 days, respectively, as shown in Fig. 1. All interferometric pairs have a perpendicular baseline of less than 150 m, thanks to the improved S1's orbital tube. The image acquired on July 31, 2017, was set as the master image to mitigate the decorrelation effect.

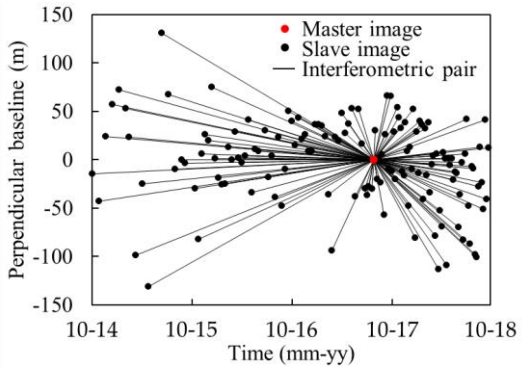

Fig. 1 S1 SAR dataset. The vertical and horizontal axes represent the perpendicular and temporal baselines of interferometric pairs.

4. METHODS

4.1 Advanced Time Series InSAR Analysis

The S1 SAR images were processed following a two-staged processing workflow, namely (1)

multiple differential interferogram formation and (2) time series InSAR analysis, as shown in Fig. 2. In Stage 1, the SeNtinel Application Platform (SNAP), freely distributed by ESA, was utilized, whereas, in Stage 2, the open-source software package of Stanford Method for Persistent Scatterers (StaMPS) was used [24].

4.1.1 Stage 1: SNAP pre-processing

First, a master image from the S1 SAR dataset is selected under good weather conditions. To this aim, the InSAR Stack Overview tool in SNAP was used. Then, the open-source snap2stamps package tool automated the pre-processing steps [25]. The area of interest (AOI) was selected during the image splitting and orbit file correction to reduce the computational effort. Subsequently, the interferogram formation followed immediately after the coregistration of slave images to the geometry of the master image using back-geocoding with Enhanced Spectral Diversity (ESD). Afterward, the Shuttle Radar Topography Mission digital elevation model (SRTM DEM) 1 arcsec data in the SNAP library allowed topographic phase removal. Then, debursting of the coregistered images and differential interferograms followed to produce seamless image products. These products are then exported in Stage 2.

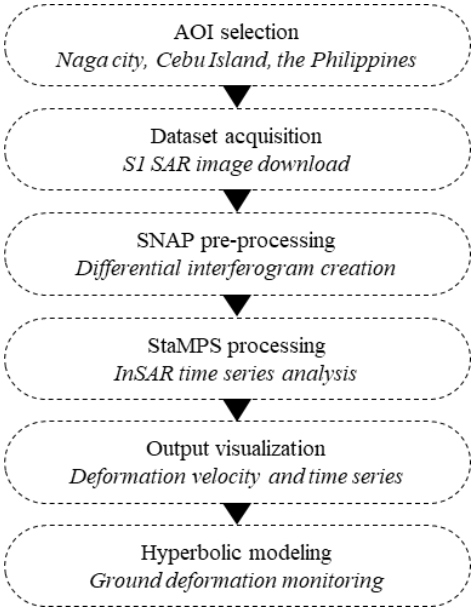

Fig. 2 General workflow of the satellite-based ground deformation monitoring over Naga city, Cebu Island in the Philippines.

4.1.2 Stage 2: StaMPS processing

After exporting the SNAP pre-processed image products into the format supported for StaMPS processing in Matlab, an amplitude dispersion index (ADI) of 0.42 was used to select and load initial PS candidates (PSCs). Then, the phase noise value for each PSC in every differential interferogram was estimated iteratively. Based on the estimated phase noise characteristics, final PSs were selected, and those PSs deemed noisy were weeded afterward. The final PSs in the wrapped phase were then corrected for DEM error. The corrected phase information is then unwrapped using the open-source software, Statistical-Cost, Network-Flow Algorithm for Phase Unwrapping (SNAPHU) [26]. Then, the spatially correlated look angle (SCLA) error is estimated and removed from the unwrapped data. Finally, phase errors attributed to atmospheric perturbations are mitigated using spatiotemporal filters.

The immediate results after Stage 2, such as the LOS mean displacement velocity map and time series, are relative measures concerning a selected reference area. For this purpose, a preliminary S1-PSInSAR analysis with an ADI of 0.60 was performed, introducing more PSCs corrupted with noise. Then, the AOI was inspected for a stable reference area by evaluating the LOS mean displacement velocity and time series of PSs groups within a moving window with a 20-m radius. The mean velocity within the selected reference area must be between ±1 mm/yr with a nearly horizontal displacement time series. Table 1 lists the critical parameters used in Stage 2.

Table 1 List of critical parameters used in Stage 2

Parameter	Value
scla_deramp	y
unwrap_gold_n_win	8
unwrap_grid_size	10
unwrap_time_win	24
scn_time_win	50
ref_centre_lonlat	123.7574, 10.20639
ref_radius	20

4.2 Hyperbolic Modeling

Due to the success of applying and validating advanced time series InSAR using various archived SAR datasets, modeling the long-term temporal evolution of ground deformation has been possible with several mathematical functions [27]–[28]. The fitted model describing the settlement curve obtained from advanced time series InSAR is typically the hyperbolic function. Advanced time series InSAR results from existing literature utilized distributed scatterers (DSs), whose phase behavior differs from PSs. Generally, DS-based time series InSAR techniques are preferred for non-urban areas with considerable vegetation cover or when few SAR images are available. On the one hand, the PSInSAR technique is more suitable for ground deformation monitoring in urban areas. Therefore,

in this study, a two-parameter hyperbolic model was fitted to the S1-PSInSAR results to describe the nonlinear deformation phenomenon over Naga city, specifically on the reclaimed land where a multipurpose complex zone is built. The displacement d at a specific time t described by the hyperbolic model is expressed in Eq. (1), as shown below [29].

$$d = t/(\alpha + \beta t) \quad (1)$$

where α and β are the PS point-specific constants derived using regression analysis. The root-mean-squared error (RMSE) and coefficient of determination (R^2) were optimized to constraint the two constants.

5. RESULTS AND DISCUSSION

5.1 Spatial Distribution of Measurement Points

After the S1-PSInSAR processing, 5,767 quality PSs were recognized over the AOI. Figure 3 shows the LOS mean displacement velocity map.

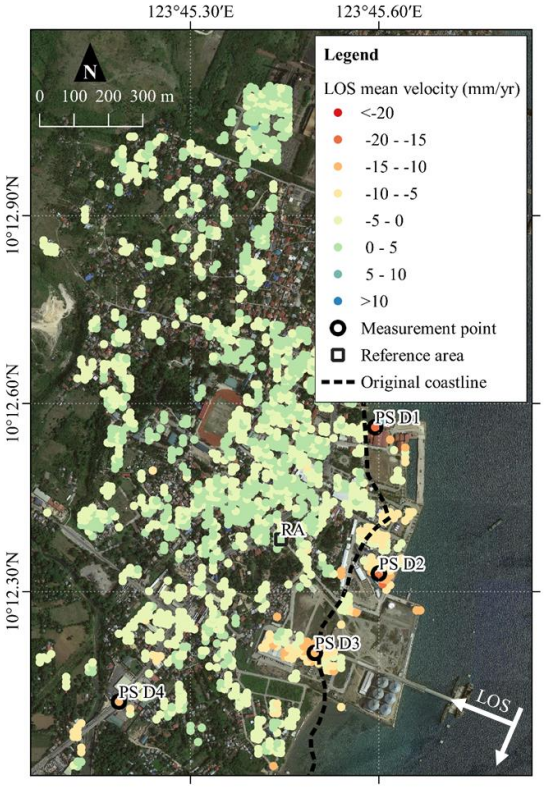

Fig. 3 LOS mean displacement velocity map over the coastal area in Naga city, Cebu Island, Philippines.

PSs were plotted relative to the selected reference stable area (i.e., negligible ground deformation). Warm colors represent a movement away from the radar (i.e., subsidence), and cold colors indicate a movement towards the radar (i.e., uplift). Most PSs were detected over built-up areas, characterized by houses, buildings, and roads. On the one hand, the complete absence of PSs over vegetated areas and water bodies is normally subjected to rapid changes between two S1 SAR image acquisitions. These rapid surface changes lead to temporal decorrelation.

Subsiding areas were detected and mapped during the analysis period over the reclaimed land, the east side of the coastline in Fig. 3, where a multipurpose complex zone is built. However, groundworks on the east side of the reclaimed land during the monitoring period resulted in a lack of PSs. The maximum subsidence rate exceeded –15 mm/yr. The inland, located west side of the coastline, was generally stable, with most of the PSs having a LOS mean displacement velocity between ±5 mm/yr. However, some PSs over the reclaimed land in Naga city, Cebu Island in the Philippines, have registered LOS mean velocity reaching –20 mm/yr. The distribution of PSs concerning the ground movement type is shown in Fig. 4.

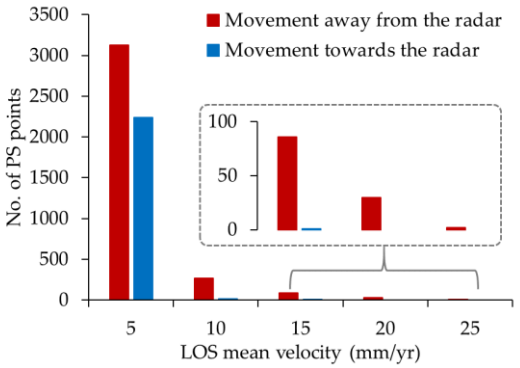

Fig. 4 Distribution of LOS mean displacement velocity for PSs over the AOI. The inset shows the number of PSs with subsidence rate ≤–15 mm/yr.

5.2 Temporal Evolution of Ground Deformation

Four representative PSs or measurement points were selected within the subsiding zone near the coastline over the AOI. These four points are labeled as PSs D1–D4 in Fig. 3. PSs D1, D2, D3, and D4 are located over the sports arena, public market, industrial flour milling company, and national road. The subsidence rate of these points exceeds –10 mm/yr. The cumulative LOS displacement time series of the PSs are plotted in Figs. 5a–d. Accumulated subsidence of the PSs varies depending on their location over the AOI. At the end of the monitoring period in September 2018,

the subsidence values of PSs D1, D2, D3, and D4 were –86.807 mm, –70.193 mm, –53.146 mm, and –45.074 mm, respectively. The maximum subsidence was recorded for PS D1, located over the reclaimed land. On the one hand, PSs recognized over the inland (i.e., PS D4) record lower subsidence values than PS D1.

The hyperbolic curve fitted to the S1-PSInSAR displacement time series of PSs D1–D4 is also plotted in Figs. 5a–d. Table 2 summarizes the optimized hyperbolic model constants. The constant α is highly dependent on the spatial location of the PSs than that of the constant β.

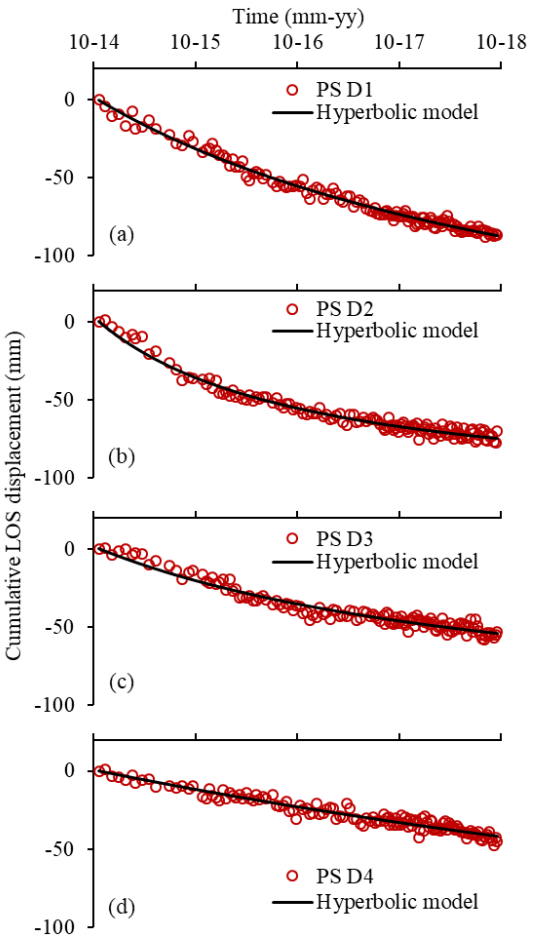

Fig. 5 Cumulative LOS displacement time series of PSs D1–D4, including the fitted hyperbolic curve for each selected monitoring points.

Table 2 Optimized hyperbolic model constants

PS No.	Model constants		RMSE	R^2
	α	β		
D1	–9.367	–0.0049	2.691	0.99
D2	–6.634	–0.0088	2.847	0.98
D3	–13.965	–0.0087	3.222	0.95
D4	–27.809	–0.0045	2.747	0.94

The modeled cumulative LOS displacements are in excellent agreement with the S1-PSInSAR results with low RMSE (<4 mm) and relatively high R^2 (>0.90). Likewise, Fig. 6 clearly shows an excellent correlation between the estimated subsidence (i.e., measured in the satellite radar LOS) at the end of the monitoring period in September 2018 using the two-parameter hyperbolic model and S1-PSInSAR measurements for 250 PSs over the AOI, including PSs D1–D4. These 250 PSs exhibit LOS mean displacement velocities between –5 mm/yr and –20 mm/yr. This excellent agreement between the S1-PSInSAR and hyperbolic model results proves that long-term monitoring and (or) forecasting of ground deformation using SAR satellite data and advanced remote sensing techniques is cost-efficient relative to traditional ground-based and terrestrial geodetic methods. Specifically, the two-parameter hyperbolic curves provide a better understanding of ground deformation's nonlinear behavior and spatiotemporal evolution over coastal cities, which are vulnerable to the effects of natural and anthropic hazards and processes.

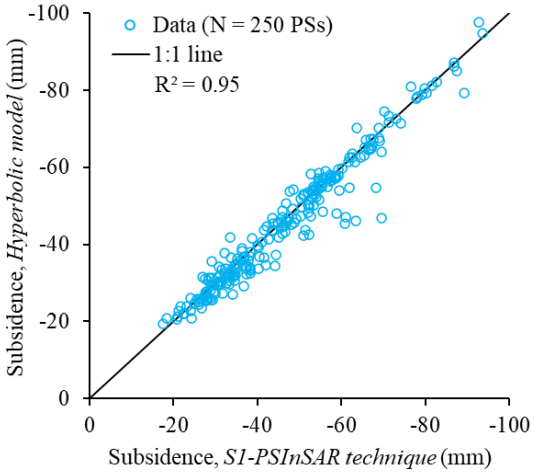

Fig. 6 The correlation between the estimated subsidence using the hyperbolic model predictions and S1-PSInSAR measurements over the AOI.

The modeled displacement time series of the four PSs implies that subsidence may have occurred before the start of the satellite-based monitoring period. However, the hyperbolic function might have yet to capture the commencement stage of the subsidence phenomenon [30]. Nevertheless, the modeled results suggest that subsidence slowly decelerates faster over time for PSs D2 and D3. For PSs D1 and D4, the modeled results suggest that stabilization is yet to occur over the coastal area. Using the Google Earth Street View function, a walkthrough over the AOI showed signs of active subsidence, such as hairline cracks on buildings, road pavements, and masonry fences (Fig. 7).

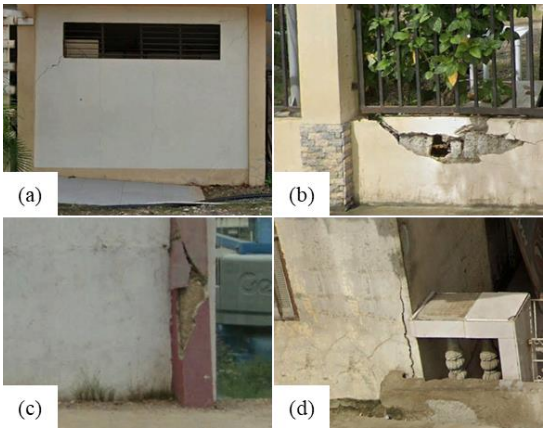

Fig. 7 Evidence of structural damage due to ground subsidence in areas encompassing (a) PS D1, (b) PS D2, (c) PS D3, and (d) PS D4.

5.3 Contributory Factors of Ground Subsidence

The modeled cumulative LOS displacement time series of PSs D1–D4 was plotted with the monthly average precipitation from October 2014 to September 2018 in Fig. 8 to verify the cause of nonlinear subsidence over the coastal area. The weather monitoring station of PAGASA in Cebu Island is located at Mactan Station (10°19'18.15"N, 123°58'33.7"E). The collected precipitation data shows a good relationship with the modeled displacement time series.

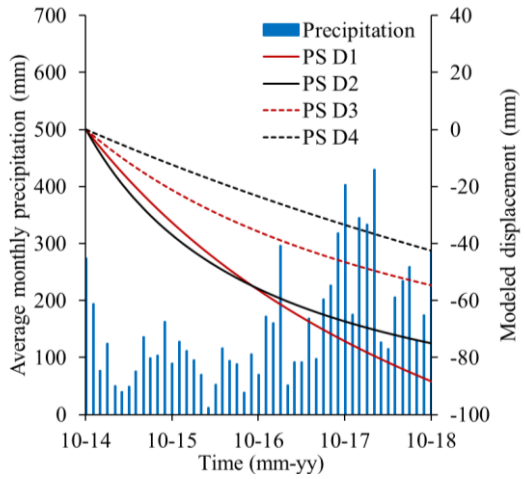

Fig. 8 Relation of modeled nonlinear cumulative LOS displacement of PSs D1–D4 with average monthly precipitation from October 2014 to September 2018.

The highest monthly average precipitations (>200 mm) were recorded between January 2017 and July 2018. In the case of PSs D2 and D3, subsidence may have decelerated after precipitation has recharged the groundwater [30]–[31]. In the case of PSs D1 and D4, subsidence may be related to precipitation and other contributory natural factors, including the geology of Naga city, the thickness of compressible soil layers along the coastal area, and the swarm of seismic activities during the monitoring period. Anthropic processes or human interventions such as excessive groundwater exploitation, continual urbanization, industrialization, and quarrying may have also contributed to the different ground deformations over the AOI. However, detailed analyses were impossible due to the lack of available ancillary data collected during the study period. Further investigation, including in-situ measurements to validate the observations, is indispensable.

Nevertheless, the S1-PSInSAR results reported here recommend continuous ground deformation monitoring until the ground has been stabilized completely. Processing archived and accessible SAR images acquired by the ascending S1 satellite can also provide additional ground deformation information over the same AOI. This information includes the directional displacement components (i.e., vertical up-down and horizontal east-west) by decomposing the LOS displacements from the ascending and descending results using the incidence and heading angles in the SAR product metadata. Displacement components might be of interest when ground deformation is not entirely vertical, which might be the case in areas near the coastline. Likewise, combining the S1-PSInSAR results obtained in this study with other available thematic information over Naga city, Cebu Island in the Philippines, improves land subsidence susceptibility and hazard mapping and zonation using sophisticated Geographic Information System (GIS)-based technologies. Moreover, the S1-PSInSAR and hyperbolic model results presented in this study need to be validated and confirmed using available in-situ measurements to prove the methods' precision and accuracy for long-term ground deformation monitoring and (or) forecasting.

6. CONCLUSIONS

This study applied the S1-PSInSAR technique and the hyperbolic function for long-term ground deformation monitoring and modeling over the coastal city of Naga in Cebu Island in the Philippines. The satellite-based SAR data and advanced remote sensing technique detected, mapped, and monitored the nonlinear ground deformation in the multipurpose complex zone built over reclaimed land. The two-parameter hyperbolic model was fitted to the S1-PSInSAR displacement time series to describe the nonlinear ground deformation behavior. Overall, the modeled results show excellent agreement with the S1-PSInSAR results, suggesting maximum ground subsidence

over –50 mm and subsidence rate over –15 mm/yr. Ground deformation over the reclaimed land continues to evolve related to natural and anthropic processes, and stabilization is yet to occur. This study suggests that the S1-PSInSAR technique and the two-parameter hyperbolic function can provide technical support in mapping, monitoring, and (or) forecasting nonlinear ground deformation over vast areas under different meteorological conditions with less human labor and efficient cost. Continuous monitoring of the ground subsidence is indispensable, and integrating other thematic information available for Naga city can provide a better understanding of the dynamic nonlinear ground deformation process.

7. ACKNOWLEDGEMENTS

The authors would like to thank the National Research Council of the Philippines (NRCP) for the financial assistance provided through the Support to Research Dissemination in Local and International Platforms (RDLIP) component of the Basic Research Information Translation for Empowerment in the Regions (BRITER) Program. The authors thank ESA and EC for freely providing S1 SAR images under the Copernicus Program and the United States Geological Survey (USGS) in cooperation with the National Aeronautics and Space Administration (NASA) for supplying the SRTM DEM 1 arcsec data. The authors also thank the Department of Civil Engineering of the University of Santo Tomas (UST) for supporting the research. The authors also thank the journal editor-in-chief and anonymous referees for their valuable and constructive comments and suggestions.

8. REFERENCES

[1] Galloway D.L., and Burbey T.J., Review: Regional Land Subsidence Accompanying Groundwater Extraction. Hydrogeology Journal, Vol. 19, 2011, pp.1459–1486.

[2] Abidin H.Z., Andreas H., Djaja R., Darmawan D., and Gamal M., Land Subsidence Characteristics of Jakarta Between 1997 and 2005, as Estimated using GPS Surveys. GPS Solutions, Vol. 12, Issue 1, 2008, pp.23–32.

[3] Pecoraro G., Calvello M., and Piciullo L., Monitoring Strategies for Local Landslide Early Warning Systems. Landslides, Vol. 16, 2019, pp.213–231.

[4] Ferretti A., Prati C., and Rocca F., Permanent Scatterers in SAR Interferometry. IEEE Transaction on Geoscience and Remote Sensing, Vol. 39, Issue 1, 2001, pp.8–20.

[5] Crosetto M., Monserrat O., Cuevas-González M., Devanthéry N., and Crippa B., Persistent Scatterer Interferometry: A Review. ISPRS Journal of Photogrammetry and Remote Sensing, Vol. 115, 2016, pp.78–89.

[6] Jia H., and Liu L., A Technical Review on Persistent Scatterer Interferometry. Journal of Modern Transportation, Vol. 24, Issue 2, 2016, pp.153–158.

[7] Peyret M., Dominguez S., Cattin R., Champenois J., Leroy M., and Zajac A., Present-day Interseismic Surface Deformation Along the Longitudinal Valley, Eastern Taiwan, from a PS-InSAR Analysis of the ERS Satellite Archives. Journal of Geophysical Research: Solid Earth, Vol. 116, Issue B3, 2011, pp.1–21.

[8] Aucelli P.P.C., Di Paola G., Incontri P., Rizzo A., Vilardo G., Benassai G., Buonocore B., and Pappone G., Coastal Inundation Risk Assessment due to Subsidence and Sea Level Rise in a Mediterranean Alluvial Plain (Volturno Coastal Plain-Southern Italy). Estuarine, Coastal and Shelf Science, Vol. 198, Issue Part B, 2017, pp.597–609.

[9] Liu P., Chen X., Li Z., Zhang Z., Xu J., Feng W., Wang C., Hu Z., Tu W., and Li H., Resolving Surface Displacements in Shenzhen of China from Time Series InSAR. Remote Sensing, Vol. 10, Issue 7, 2018, pp.1162.

[10] Polcari M., Albano M., Montuori A., Bignami C., Tolomei C., Pezzo G., Falcone S., La Piana C., Doumaz F., Salvi S., and Stramondo S., InSAR Monitoring of Italian Coastline Revealing Natural and Anthropogenic Ground Deformation Phenomena and Future Perspectives. Sustainability, Vol. 10, Issue 9, 2018, pp.3152.

[11] Hu B., Chen J., and Zhang X., Monitoring the Land Subsidence Area in a Coastal Urban Area with InSAR and GNSS. Sensors, Vol. 19, Issue 14, 2019, pp.3181.

[12] Altintas F., and Gokalp E., Monitoring Surface Deformations of the Reclamation Site using PS Interferometry: Senol Gunes Sports Complex (Turkey). Geocarto International, Vol. 37, Issue 24, 2022, pp.7247–7260.

[13] Raucoules D., Le Cozannet G., Wöppelmann G., de Michele M., Gravelle M., Daag A., and Marcos M., High Nonlinear Urban Ground Motion in Manila (Philippines) from 1993 to 2010 observed by DInSAR: Implication for Sea-level Measurement. Remote Sensing of Environment, Vol. 139, 2013, pp.386–397.

[14] Espiritu K.W., Reyes C.J., Benitez T.M., Tokita R.C., Galvez L.J., and Ramirez R., Sentinel-1 Interferometric Synthetic Aperture Radar (InSAR) Reveals Continued Ground Deformation In and Around Metro Manila, Philippines, Associated with Groundwater Exploitation. Natural Hazards, Vol. 114, 2022, pp.3139–3161.

[15] Mayuga P.J., Tiongson S.F., Abao J.J., Mendoza J.M., Pernez G.A., and Ramirez R., Landslide Area Mapping using Synthetic Aperture Radar (SAR) Data: The Case of the 2018 Naga Landslide. In Proceedings of the 2022 IEEE International Geoscience and Remote Sensing Symposium, 2022, pp.1–4.

[16] Ramirez R., The Application of Interferometric Synthetic Aperture Radar (InSAR) on Damaged Area Mapping: The Case of the 2020 Taal Volcano Eruption. In Proceedings of the 2021 IEEE International Geoscience and Remote Sensing Symposium, 2021, pp.1–4.

[17] Ramirez R.A., and Abdullah R.E.E., Damaged Area Mapping and Ground Displacement Estimation using Sentinel-1 Synthetic Aperture Radar (SAR) Interferometry: January 12, 2020, Taal Volcano Eruption Case Study, Philippines. Mindanao Journal of Science and Technology, Vol. 20, Issue 2, pp.1–27.

[18] Abcede E.L., Ajesta A., Alfonso J.D., Nucup R.J., Peralta M., and Ramirez R., InSAR-based Detection and Mapping of Seismically Induced Ground Surface Displacement and Damage in Pampanga, Philippines. ASEAN Engineering Journal, Vol. 12, Issue 2, 2022, pp.1–10.

[19] Tiongson S.F., and Ramirez R., Mapping of Ground Surface Deformations and Its Associated Damage using SAR Interferometry: A Case Study of the 2020 Masbate Earthquake. E3S Web of Conferences, Vol. 347, In Proceedings of the 2nd International Conference on Civil and Environmental Engineering, 2022, pp.03014.

[20] Dimalanta C., Suerte L., Yumul G., Tamayo R., and Ramos E., A Cretaceous Supra-Subduction Oceanic Basin Source for Central Philippine Ophiolitic Basement Complexes: Geological and Geophysical Constraints. Geosciences Journal, Vol. 10, Issue 3, 2006, pp.305–320.

[21] Deng J., Yang X., Zhang Z.F., and Santosh M., Early Cretaceous Arc Volcanic Suite in Cebu Island, Central Philippines and Its Implications on Paleo-Pacific Plate Subduction: Constraints from Geochemistry, Zircon U-Pb Geomorphology and Lu-Hf Isotopes. Lithos, Vol. 230, 2015, pp.166–179.

[22] Beck H.E., Zimmermann N.E., McVicar T.R., Vergopolan N., Berg A., and Wood E.F., Present and Future Köppen-Geiger Climate Classification Maps at 1-km Resolution. Scientific Data, Vol. 5, 2018, pp.108214.

[23] Torres R., Snoeij P., Geudtner D., Bibby D., Davidson M., Attema E., Potin P., Rommen B., Floury N., Brown M., Traver I.N., Deghaye P., Duesmann B., Rosich B., Miranda N., Bruno C., L'Abbate M., Croci R., Pietropaolo A., Huchler M., and Rostan F., GMES Sentinel-1 Mission. Remote Sensing of Environment, Vol. 120, 2012, pp.9–24.

[24] Hooper A., Bekaert D., Spaans K., and Arikan M., Recent Advances in SAR Interferometry Time Series Analysis for Measuring Crustal Deformation. Tectonophysics, Vol. 514–514, 2012, pp.1–13.

[25] Foumelis M., Delgado Blasco J.M., Desnos Y.L., Engdahl M., Fernández D., Veci L., Lu L., and Wong C., ESA SNAP-StaMPS Integrated Processing for Sentinel-1 Persistent Scatterer Interferometry. In Proceedings of the 2018 IEEE International Geoscience and Remote Sensing Symposium, 2018, pp.1364–1367.

[26] Chen C.W., and Zebker H.A., Two-dimensional Phase Unwrapping with Use of Statistical Models for Cost Functions in Nonlinear Optimization. Journal of the Optical Society of America A, Vol. 18, Issue 2, 2001, pp.338–351.

[27] Kim S.W., and Won J.S., Measurements of Soil Compaction Rate by using JERS-1 SAR and a Prediction Model. IEEE Transactions on Geoscience and Remote Sensing, Vol. 41, Issue 11, 2003, pp.2683–2686.

[28] Park S.W., and Hong S.H., Nonlinear Modeling of Subsidence from a Decade of InSAR Time Series. Geophysical Research Letters, Vol. 48, Issue 3, 2021, pp.1–10.

[29] Tan T.S., Inoue T., and Lee S.L., Hyperbolic Method for Consolidation Analysis. ASCE Journal of Geotechnical Engineering, Vol. 117, Issue 11, 1991, pp.1723–1737.

[30] Zhang Y., Liu Y., Jin M., Jing Y., Liu Y., Liu Y., Sun W., Wei J., and Chen Y., Monitoring Land Subsidence in Wuhan City (China) using the SBAS-InSAR Method with Radarsat-2 Imagery Data. Sensors, Vol. 19, Issue 3, 2019, pp.743.

[31] Zhou L., Guo J., Hu J., Li J., Xu Y., Pan Y., and Shi M., Wuhan Surface Subsidence Analysis in 2015–2016 based on Sentinel-1A Data by SBAS-InSAR. Remote Sensing, Vol. 9, Issue 10, 2017, pp.982.